

Electrical double-layer capacitors with plasticized polymer electrolyte based on methyl cellulose

N. E. A. Shuhaimi · L. P. Teo · H. J. Woo ·
S. R. Majid · A. K. Arof

Received: 2 December 2011 / Revised: 17 April 2012 / Accepted: 3 May 2012 /
Published online: 13 May 2012
© Springer-Verlag 2012

Abstract Poly(ethylene glycol) plasticized polymer electrolytes based on methyl cellulose have been prepared using the solution casting technique. Interactions between component materials in the electrolyte have been examined using Fourier transform infrared spectroscopy. The polymer-salt spectrum indicates that interaction occurred at the oxygen atom with the shift of the C–O stretching mode. Inference from the Nyquist plot suggests that the material can be represented by a resistor connected in series with a constant phase element. Capacitance evaluated from the fitting equation representing impedance of the equivalent circuit is observed to decrease with increasing temperature. From linear sweep voltammogram, the 63.75 wt% MC-21.25 wt% NH_4NO_3 -15 wt% PEG, which is the highest conducting plasticized sample shows good electrochemical stability. This material has been tested as an electrolyte in electrical double-layer capacitor fabricated in this study. The electrochemical properties of the capacitors have been investigated by cyclic voltammetry, charge-discharge, and self-discharge characteristics. The discharge capacitance obtained is 38 F g^{-1} .

Keywords Methyl cellulose · NH_4NO_3 · PEG · Electrolyte · FTIR · EIS · EDLC

Introduction

Electrical double-layer capacitor (EDLC) is one type of supercapacitors that consists of a pair of polarizable electrodes and does not exhibit Faradaic reactions over the potential range of operation [1]. The mechanism of EDLC is based on the phenomenon that an electric double-layer is formed at the boundary between the

N. E. A. Shuhaimi · L. P. Teo · H. J. Woo · S. R. Majid · A. K. Arof (✉)
Centre for Ionics University of Malaya, Department of Physics, Faculty of Science,
University of Malaya, 50603 Kuala Lumpur, Malaysia
e-mail: akarof@um.edu.my

electrode and electrolyte [2]. Since no electrochemical reaction occurred, EDLC is an environmental friendly device. Although EDLCs are commercially available in the market, they use liquid electrolytes. Liquid electrolyte has many disadvantages such as being leak-prone, corrosive, and devices using liquid electrolyte may be bulky with high self-discharge rate. The use of liquid electrolytes also incurs high cost because of the need of a separator to prevent electrode-electrode contact.

To overcome the problem, high-conducting polymer electrolytes with good mechanical strength, electrochemical stability, low cost, and compatible with electrode materials are being developed. Poly(ethylene oxide), PEO, introduced by Wright and co-researchers in the seventies is the state of the art host polymer in polymer electrolyte research. PEO has high concentration of crystalline phases and thus when complexed with a salt exhibits low ionic conductivity. Hence, other polymers were investigated to replace PEO. Examples include poly(methyl methacrylate) (PMMA), poly(vinyl alcohol) (PVA), poly(acrylonitrile) (PAN), and poly(vinyl chloride) (PVC). Methyl cellulose (MC) has also been used as a polymer host in the preparation of polymer electrolytes [3–5]. MC is a water soluble polysaccharide that consists of β (1 \rightarrow 4) glucosidic units with methyl substituent in linear chains [6]. It can be prepared from the reaction of alkali-cellulose with dimethyl sulfate or methyl chloride [7]. According to some reports MC is an amorphous polymer [8, 9] while others claimed that MC is semi-crystalline [10]. Among biodegradable polymers, MC has good mechanical strength [11], and excellent film forming ability [12]. It is also cheap and non-toxic, but most importantly, it has lone pair electrons at its oxygen atoms where cation of a salt can loosely interact with the polymer. These features serve as motivation in the study of polymer electrolytes based on MC.

Based on our previous work [3–5], the sample 75 wt% MC-25 wt% NH_4NO_3 exhibits a room temperature conductivity of $2.1 \times 10^{-6} \text{ S cm}^{-1}$. This value, if not better, is comparable to other systems such as poly(vinyl pyrrolidone)-ammonium acetate ($1.5 \times 10^{-6} \text{ S cm}^{-1}$) [13], PEO- NH_4F ($1.1 \times 10^{-6} \text{ S cm}^{-1}$) [14], and PEG₄₆- NH_4ClO_4 ($2.7 \times 10^{-6} \text{ S cm}^{-1}$) [15]. Although the conductivity is comparable with literature reports for solid polymer electrolytes (SPEs) doped with ammonium salt, $\sim 10^{-6} \text{ S cm}^{-1}$ but it is still insufficient for application in electrochemical devices such as EDLC. Hence, in this work we have plasticized 75 wt% MC-25 wt% NH_4NO_3 with poly(ethylene glycol) of molecular weight 200 g mol^{-1} (PEG200) to enhance conductivity value and use the membrane in EDLC fabrication. Results will be presented, discussed, and compared with reports found in the literature.

Experimental details

Polymer electrolyte preparation

MC-based polymer electrolytes were prepared using the solution casting technique. MC, procured from Sigma-Aldrich M0512 (viscosity 4 000 cP in 2 % aqueous solution at 20 °C), liquid poly(ethylene glycol) of molecular weight, 200 g mol^{-1}

PEG200, was procured from Sigma-Aldrich P3015 and NH_4NO_3 from Ajax were all used as received. Details of sample preparation have been reported elsewhere [3–5]. To the highest conducting MC– NH_4NO_3 system, PEG200 was added and the composition optimized for highest room temperature conductivity.

X-ray diffraction (XRD)

X-ray diffraction patterns have been obtained using Siemens D5000 X-ray diffractometer in the 2θ range from 5° to 80° using Cu-K α radiation. Operating current was 40 mA and operating voltage was 40 kV. The diffractogram of 75 wt% MC–25 wt% NH_4NO_3 electrolyte was compared with that of 63.75 wt% MC–21.25 wt% NH_4NO_3 –15 wt% PEG electrolyte. These samples have the highest conducting electrolyte in the unplasticized and plasticized systems.

Fourier transform infrared (FTIR) spectroscopy

FTIR spectroscopy was carried out to determine polymer-salt complexation and to examine interaction(s) between component materials in the sample. The FTIR spectrum of pure MC, pure NH_4NO_3 , pure PEG, MC– NH_4NO_3 , MC-PEG, PEG– NH_4NO_3 , and MC– NH_4NO_3 -PEG were recorded using the Thermo Scientific (Nicolet iS10) spectrophotometer from 4,000 to 650 cm^{-1} with resolution 1 cm^{-1} at room temperature. Each spectrum runs 32 scans with correction against the background spectrum of air. Dry nitrogen was used for purging purposes in order to exclude the infrared active H_2O and CO_2 in the atmosphere.

EIS measurements

EIS measurements on the MC– NH_4NO_3 and MC– NH_4NO_3 -PEG samples were carried out using the HIOKI 3531-01 LCR bridge in the frequency range 50 Hz to 1 MHz and in the temperature range from 298 to 373 K. The voltage amplitude was 10 mV. Before measurement, the samples were continuously dried in desiccators for a few days. Following Qian et al. [16] blocking electrodes were used in a two-electrode cell configuration to determine the bulk resistance of electrolytes. In this study, stainless steel (SS) electrodes were used as blocking electrodes and the samples were sandwiched between them. SS blocks ion transport and is an inert electrode for the polymer electrolyte. This insures the non-occurrence of passivation phenomenon [17]. Thickness of the polymer electrolyte samples is $<100\text{ }\mu\text{m}$. The impedance data were displayed in a Nyquist plot.

Linear sweep voltammetry (LSV)

Before applying the membrane in EDLC, the electrochemical stability window of the sample was investigated using the Autolab PGSTAT 12 potentiostat/galvanostat in conjunction with the General Purpose Electrochemical System (GPES) software Version 4.9.005. The sample was sandwiched between stainless steel electrodes.

The scan rate was 1 mV s^{-1} and the potential applied was in the range from -2.5 to 2.5 V . The experiment was done at room temperature.

Electrode preparation

Normally the materials to prepare electrodes consist of a carbonaceous active material, binder and solvent. 81 wt% activated carbon (BP20) purchased from Kuraray Chemical Co., LTD was used as carbonaceous material. This carbon is based on phenol resin and has total surface area between $1,700$ and $1,800 \text{ m}^2 \text{ g}^{-1}$. The particle size is between 2 and $20 \mu\text{m}$ in diameter. 6 wt% carbon black (CB), which is also an activated carbon, was added to the mixture of BP20 and *N*-methyl-2-pyrrolidone (NMP). CB has been reported to reduce internal resistance of the electrodes [2]. According to Latham et al. [18], CB can also be used to improve the contact between electrode and electrolyte. In this study, MC was used as binder in the electrode following Chang et al. [19] and Bispo-Foncesca et al. [20]. 13 wt% MC was added in the electrode material but it was first dissolved in NMP. The mixture was stirred until homogeneous. In this study, the electrode was prepared using dip-coating method. Aluminum grid was used as current collector on which the electrode was coated. Aluminum grid was washed using ethanol prior to use. Apart from the activated carbon, binder and solvent, some polymer electrolyte was also added in liquid form to the electrode slurry.

Preparation of EDLC

The EDLC assembly is shown in Fig. 1. The electrode area was 4.5 cm^2 . The 63.75 wt% MC-21.25 wt% NH_4NO_3 -15 wt% PEG electrolyte-cum-separator was sandwiched between two identical carbon electrodes. The electrode/electrolyte/electrode conjugate was clamped between rectangular Perspex plates to form the EDLC. Two EDLC cells were prepared. In one, the electrodes were coated with a

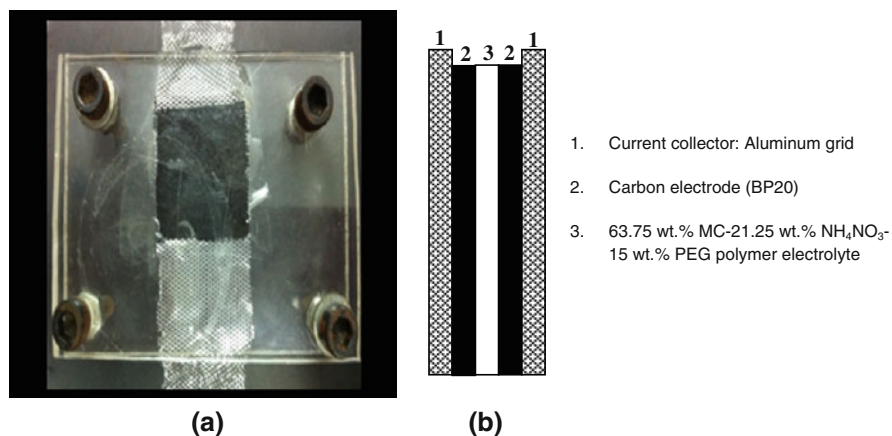


Fig. 1 a Photograph of the fabricated EDLC. b Schematic representation of the side view of EDLC

PEG layer and in the other, the electrodes were without the PEG coating. The thickness of the PEG layer is at most ~ 70 μm .

Cyclic voltammetry (CV)

The capacitor performance was investigated using CV test. CV was performed using the Autolab PGSTAT 12 potentiostat/galvanostat in conjunction with the General Purpose Electrochemical System (GPES) software Version 4.9.005. The scan rate was 1 mV s^{-1} in the sweep region 0–0.85 V at room temperature.

Charge-discharge and self-discharge characteristics

The charge-discharge and self-discharge characteristics were carried out using the Neware battery cyler. For charge-discharge characteristics, the working voltage applied to EDLC was 0.85 V and the current was 1 mA. For self-discharge characteristics, the EDLC was first charged to 0.85 V, then discharged to 0 V and charged again to 0.85 V at a constant current 1 mA. The open circuit voltage was monitored for 2 h. All measurements were performed at room temperature.

Results and discussion

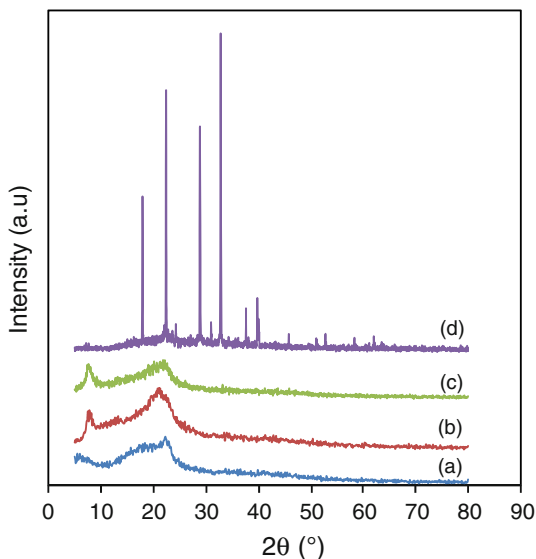
X-ray diffraction (XRD)

X-ray diffractogram of pure MC, 75 wt% MC-25 wt% NH_4NO_3 , 63.75 wt% MC-21.25 wt% NH_4NO_3 -15 wt% PEG and pure NH_4NO_3 are shown in Fig. 2. The diffractogram of pure MC film and pure NH_4NO_3 did not show any peak at $2\theta = 8^\circ$. After addition of various concentrations of NH_4NO_3 from 5 to 30 wt%, it can be observed that, a new peak appeared at $2\theta = 8^\circ$. The diffractograms for all MC- NH_4NO_3 samples have been reported in our previous papers [3–5]. This peak at $2\theta = 8^\circ$ indicates interaction between polymer and salt and it also exists in the diffractogram of samples containing PEG200. Kolhe and Kannan [21] have also shown the diffractogram of PEG (molecular weight $10,000 \text{ g mol}^{-1}$) which do not show any peak at $2\theta = 8^\circ$.

FTIR analysis

The functional groups were identified by monitoring the vibrational modes that are essentially the fingerprint of the materials under study [22]. The vibrational modes of pure MC, pure NH_4NO_3 , and pure PEG are listed in Table 1. The vibrational modes of pure MC agrees well with that reported in the literature [7, 9, 12, 23–25]. The assignments for pure NH_4NO_3 are also comparable with Ramya et al. [26], Majid [27], Hashmi et al. [28], Singh et al. [29], and Marinković et al. [30]. The positions of the bands for pure PEG are also located at wavenumber positions similar to that reported in the literature [31–33].

Fig. 2 X-ray diffractogram for **a** pure MC film, **b** 75 wt% MC-25 wt% NH_4NO_3 , **c** 63.75 wt% MC-21.25 wt% NH_4NO_3 -15 wt% PEG, and **d** pure NH_4NO_3



The interactions between host polymer (MC), salt (NH_4NO_3), and plasticizer (PEG) were also investigated using FTIR spectroscopy. Figure 3 displays the infrared spectra for pure MC, pure NH_4NO_3 , binary system-containing 75 wt% MC-25 wt% NH_4NO_3 to determine interaction between polymer and salt, pure PEG, 75 wt% MC-25 wt% PEG to determine interaction between polymer and plasticizer, 95 wt% PEG-5 wt% NH_4NO_3 to determine interaction between salt and plasticizer and the plasticized sample-containing 63.75 wt% MC-21.25 wt% NH_4NO_3 -15 wt% PEG in the wave numbers region from 650 to $1,310\text{ cm}^{-1}$. Pure MC, Fig. 3(i) shows the vibrational mode of C–O stretching at $1,053\text{ cm}^{-1}$. After addition of 25 wt% NH_4NO_3 , the band shifted to $1,051\text{ cm}^{-1}$ indicating interaction between the NH_4^+ cation and oxygen atom in C–O bond of MC as shown in Fig. 3(iii). The oxygen atom acts as electron donor as it possesses lone pair electrons. This, in fact increases amorphousness of the polymer electrolyte enabling continuous motion of the charge carriers that led to a maximum conductivity of $2.1 \times 10^{-6}\text{ S cm}^{-1}$ for the 75 wt% MC-25 wt% NH_4NO_3 polymer-salt binary system.

Before studying the effect of PEG plasticizer on 75 wt% MC-25 wt% NH_4NO_3 system, interaction between PEG and polymer and between PEG and the salt, were investigated. As can be seen in Fig. 3(v), the spectrum of 75 wt% MC-25 wt% PEG, shows a peak at $1,057\text{ cm}^{-1}$. This peak could have been formed due to the merger of peaks at $1,053\text{ cm}^{-1}$ (in the spectrum of pure MC) and at $1,061\text{ cm}^{-1}$ (in the spectrum of pure PEG), which have disappeared.

In the spectrum of 95 wt% PEG-5 wt% NH_4NO_3 , the $1,061\text{ cm}^{-1}$ band of C–O–C vibrational mode shifted to $1,063\text{ cm}^{-1}$ as shown in Fig. 3(vi). This is attributed to the interaction between the ether group oxygen in PEG and the NH_4^+ cation of the salt. Hence, from these results it can be inferred that ion transport occurs between the oxygen atoms in MC from the shift of the C–O band at $1,053$ – $1,051\text{ cm}^{-1}$ and between the oxygen atoms in PEG due to the shift in the

Table 1 Vibrational modes (obtained in this study) and the corresponding assignments for pure MC, pure NH_4NO_3 , and pure PEG

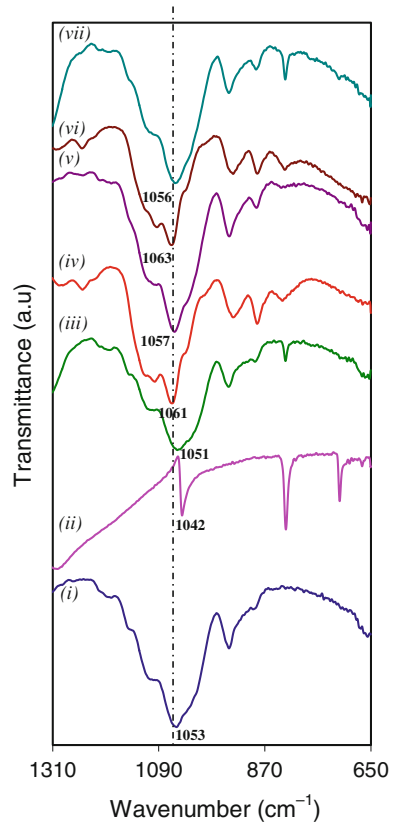
| Wavenumber (cm^{-1}) | | | Assignment as vibrational modes |
|---------------------------------|--------------------------|-------|--|
| MC | NH_4NO_3 | PEG | |
| – | 715 | – | NO_2 bending |
| – | 827 | – | Free ions of NO_3^- |
| – | – | 833 | The infrared spectral characterization for PEG ²¹ |
| – | – | 885 | The infrared spectral characterization for PEG ²¹ |
| – | – | 936 | C–O–C stretching |
| 944 | – | – | The infrared spectral characterization for MC ⁷ |
| – | 1,042 | – | NO_2 stretching |
| 1,053 | – | – | C–O stretching |
| – | – | 1,061 | C–O–C stretching |
| – | – | 1,098 | C–O–C stretching |
| 1,112 | – | – | C–O stretching |
| 1,152 | – | – | C–O stretching |
| – | – | 1,247 | C–O–C stretching |
| – | 1,300 | – | Symmetric of NO_2 stretching |
| – | – | 1,349 | C–O–C stretching |
| 1,374 | – | – | C–H bending |
| – | 1,407 | – | N–H bending |
| – | 1,419 | – | NO_2 stretching |
| – | – | 1,452 | C–O–C stretching |
| 1,458 | – | – | The infrared spectral characterization for MC ⁷ |
| 1,580–1,700 | – | – | Bending mode of water molecule |
| – | 1,754 | – | NH_4^+ stretching |
| 2,838 | – | – | C–H stretching |
| – | – | 2,867 | CH_2 stretching |
| 2,902 | – | – | C–H stretching |
| – | 3,058 | – | N–H stretching |
| – | 3,236 | – | N–H stretching |
| – | – | 3,403 | O–H stretching |
| 3,440 | – | – | O–H stretching |

C–O–C band from 1,061 to 1,063 cm^{-1} . This implies that PEG can serve as transit site for ion conduction in the plasticized MC– NH_4NO_3 –PEG system. In this system, the ion will require lesser energy for conduction [4] and the conductivity enhanced to $1.14 \times 10^{-4} \text{ S cm}^{-1}$. More details will be explained in next section.

EIS analysis and equivalent circuit model

The room temperature ionic conductivity of unplasticized electrolytes as a function of salt concentration and MC– NH_4NO_3 polymer electrolytes as a function of PEG concentration are displayed in Fig. 4.

Fig. 3 FTIR spectrum at room temperature of (i) pure MC, (ii) pure NH_4NO_3 , (iii) 75 wt% MC-25 wt% NH_4NO_3 , (iv) pure PEG, (v) 75 wt% MC-25 wt% PEG, (vi) 95 wt% PEG-5 wt% NH_4NO_3 , (vii) 63.75 wt% MC-21.25 wt% NH_4NO_3 -15 wt% PEG



The ionic conductivity increases with increase of NH_4NO_3 concentration up to 25 wt% and decreases on further increase in salt concentration. The increase in the ionic conductivity with increasing salt content can be related to the increase in the number density of mobile charge carriers as explained in our previous paper [4]. Since the conductivity is insufficient for device application, low molecular weight PEG, $M_r = 200$, was chosen as plasticizer in order to enhance the conductivity. According to Park and Ruckestein [11], among the many plasticizers for MC, PEG is the most suitable for the preparation of proton conducting electrolytes. Since it can retain moderate moisture in the polymer and improves membrane flexibility without decreasing its mechanical strength. According to Ayranci and Tunç [34], PEG can reduce brittleness and increase flexibility, toughness, and tear resistance of edible films. However, increasing PEG content also increases water vapor permeability of the films. PEG plasticizer has various molecular weights, i.e., 200, 400, and 600 g mol^{-1} . Park et al. [35] investigated relative permittivity and viscosity effects of PEG on room temperature conductivity and showed that low molecular weight PEG has higher relative permittivity and lower viscosity, which makes low molecular weight PEG more suitable for conductivity enhancement. Subban and co-researchers [36] also reported that PEG200 is a better plasticizer compared to the heavier molecular weight PEGs. Pradhan et al. [37] reported that plasticizing 95 wt% $(\text{PEO})_{25}\text{NaI}$ -5 wt%

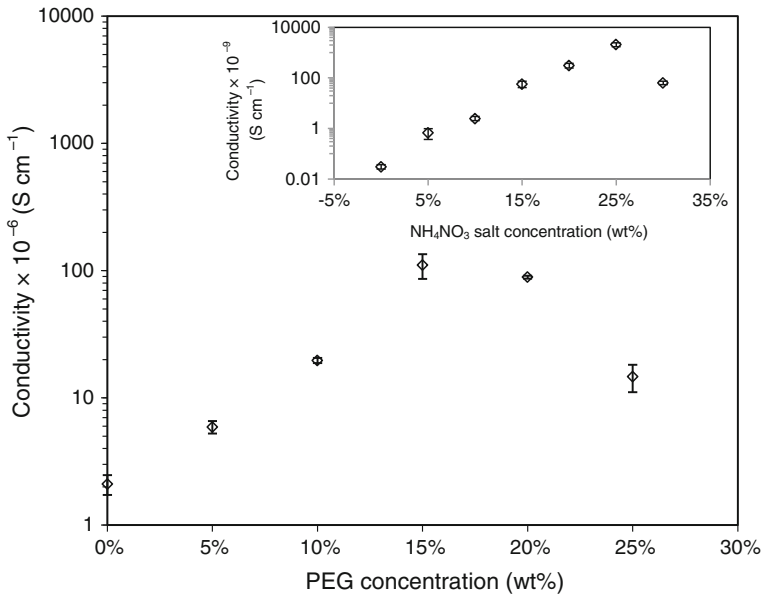


Fig. 4 Room temperature ionic conductivity of plasticized MC–NH₄NO₃ polymer electrolyte. *Inset* for unplasticized MC–NH₄NO₃ polymer electrolyte

DMMT composite polymer electrolyte with PEG200 enhanced the electrical conductivity by one order of magnitude at room temperature. DMMT stands for dodecyl amine modified montmorillonite. Srivastava and Chandra [38] prepared proton conducting polymer system based on poly(ethylene succinate) doped with NH₄ClO₄ and its conductivity is higher for plasticized sample using PEG200. The presence of PEG has resulted in new conducting pathways for the mobile ions.

Figure 5 depicts the Nyquist plots for 63.75 wt% MC-21.25 wt% NH₄NO₃-15 wt% PEG sample at various temperatures. In this experiment, only a spike was observed in the Nyquist plots for all temperatures studied, indicating that the current carriers are ions and the total conductivity is mainly the result of ion conduction [22]. Wu et al. [39] stated that, a straight line parallel to the imaginary axis in the low frequency region is caused by the effect of blocking electrodes and is also attributed to the non-homogeneity or roughness of the electrode-electrolyte interface.

When an a.c. signal is applied to the system, the impedance, Z is defined as the ratio of the voltage to the current at a given frequency and consists of a real part, Z' and an imaginary part, Z'' with phase angle, θ [40]. Since EIS is based on Fourier transformation and only defined in linear systems theory, the impedance is expressed as a complex number:

$$Z_{(j\omega)} = Z' - jZ''$$

where Z' is the real component and Z'' is the imaginary component. The parameter j is $\sqrt{-1}$. In an alternate form, $Z_{(j\omega)} = |Z| e^{j\phi}$, where $|Z| = \sqrt{(Z')^2 + (Z'')^2}$. $\theta = \tan^{-1}(\frac{Z''}{Z'})$.

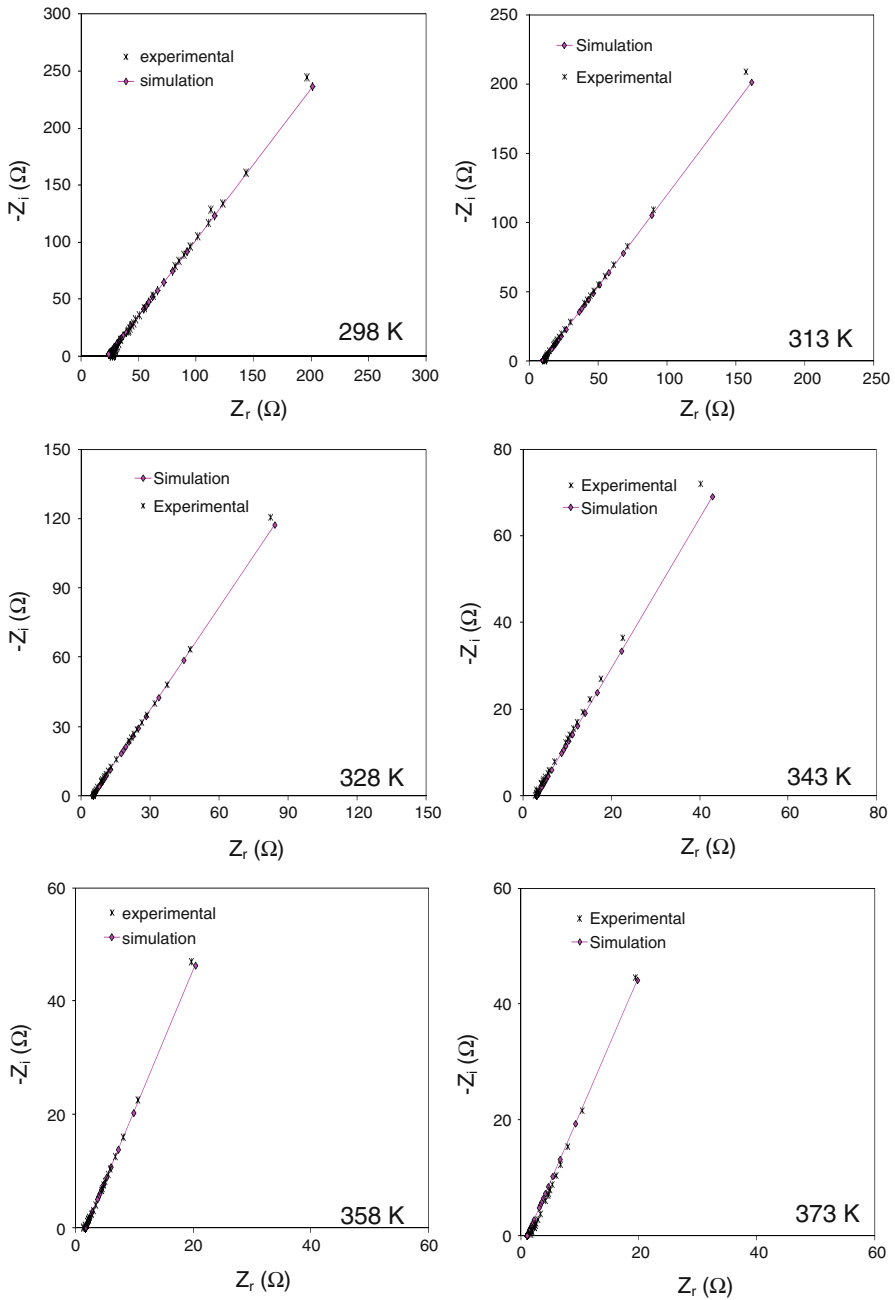


Fig. 5 Nyquist plot for 63.75 wt% MC-21.25 wt% NH_4NO_3 -15 wt% PEG sample at various temperatures

According to Han and Choi [41], the equivalent circuit is an effective way to analyse the impedance data because it is fast, simple and provides the complete picture of the system. Since the spike in this study did not begin at the origin, the equivalent circuit is implied to consist of a resistor and constant phase element (CPE) in series connection as shown in Fig. 6.

CPE can be assumed as a leaky capacitor, to compensate for inhomogeneity in the sample [16]. CPE for the spike is due to the double-layer capacity of an inhomogeneous electrode surface. In this paper, the equivalent impedance for the 63.75 wt% MC-21.25 wt% NH_4NO_3 -15 wt% PEG highest conducting plasticized sample can be expressed with the resistance, R (due to electrolyte) in series with the CPE impedance, Z_{cpe} which can be expressed as:

$$Z_{\text{total}} = R + \frac{k}{\omega^p} [\cos(p\pi/2) - j \sin(p\pi/2)]$$

The second-term on the right-hand side represents the impedance of the constant phase element, Z_{cpe} . Here k is C^{-1} the inverse of capacitance, C and p is related to the deviation of the spike from the horizontal axis. When $p = 1$, $Z_{\text{total}} = R - \frac{j}{\omega C}$. When $p = 0$, the constant phase element is a perfect resistor, Z_{total} is frequency independent. When $0 < p < 1$, CPE acts in a way intermediate between a resistor and a capacitor. When $p = 0.5$, the impedance is known as Warburg impedance.

Using the equivalent circuit, the impedance data was analyzed by superimposing the best fit of the dispersion data by trial and error. As shown in Fig. 5, the impedance of the assumed equivalent circuit fits the experimental impedance data very well. Table 2 lists the value for the circuit elements of the sample together with its conductivity.

The electrode-electrolyte interface can be considered as a double-layer if blocking electrodes were used in the impedance measurement [39]. The spike in this study is inclined at an angle $<90^\circ$ and the value of p lies between 0 and 1. This reveals that the samples have a resistive and capacitive behavior. From Table 2, it can be observed that, the value of p increases as temperature increases from 298 to 373 K. It is obvious that, the sample becomes more capacitive than resistive as temperature increases. The bulk resistance, which was obtained from the intercept of the plot with the real impedance axis decreases when temperature increases. The decrease in bulk resistance enhances conductivity and conductivity increases with temperature. Ramya et al. [26] reported that the spike is characteristic of a blocking double-layer capacitance and should be of the order of μF . The capacitance is due to electrode polarization. The value of capacitance obtained from simulation studies in this study is comparable with the results as reported in the literature [26]. The capacitance is also observed to increase with temperature up to 343 K implying suitability for use in EDLC.

Fig. 6 Equivalent circuit

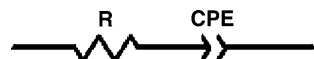


Table 2 Parameter for circuit elements

| Temperature (K) | R_b (Ω) | σ ($\times 10^{-4}$ S cm $^{-1}$) | k ($\times 10^3$ F $^{-1}$) | C ($\times 10^{-6}$ F) | p (rad) |
|-----------------|--------------------|--|---------------------------------|---------------------------|-----------|
| 298 | 23.13 | 1.10 | 8.80 | 113.64 | 0.59 |
| 303 | 14.77 | 1.85 | 10.20 | 98.04 | 0.59 |
| 308 | 11.77 | 2.28 | 8.70 | 114.94 | 0.59 |
| 313 | 9.40 | 3.04 | 7.50 | 133.33 | 0.59 |
| 318 | 7.40 | 3.61 | 6.10 | 163.93 | 0.59 |
| 323 | 5.22 | 5.16 | 5.85 | 170.94 | 0.61 |
| 328 | 4.97 | 5.27 | 5.30 | 188.68 | 0.63 |
| 333 | 4.13 | 6.25 | 4.30 | 232.56 | 0.63 |
| 338 | 3.18 | 8.17 | 4.16 | 240.38 | 0.66 |
| 343 | 2.93 | 8.72 | 3.55 | 281.69 | 0.66 |
| 348 | 2.30 | 10.60 | 3.65 | 273.97 | 0.66 |
| 353 | 1.85 | 13.10 | 4.45 | 224.72 | 0.72 |
| 358 | 1.65 | 16.00 | 3.73 | 268.10 | 0.75 |
| 363 | 1.27 | 19.80 | 4.15 | 240.96 | 0.75 |
| 368 | 1.23 | 22.30 | 3.40 | 294.12 | 0.75 |
| 373 | 1.00 | 24.40 | 3.58 | 279.33 | 0.75 |

Linear sweep voltammetry

Figure 7 depicts linear sweep voltammogram for the highest conducting plasticized MC–NH₄NO₃ polymer electrolyte. From the figure, it can be seen that the current onset is detected at 2.4 V for the plasticized sample, 63.75 wt% MC–21.25 wt% NH₄NO₃–15 wt% PEG. The current onset is assumed to be the polymer electrolyte film breakdown voltage [42]. To test performance of any device, the electrochemical stability of the sample must be known prior to charge-discharge cycling test. The breakdown voltage is important to prevent the electrolyte from being destroyed. Since in this study, the working voltage used was 0.85 V, the electrolytes should be electrochemically stable for use in the EDLCs.

Cyclic voltammetry

To understand the performance of EDLC such as electrochemical behavior and the nature of charge storage at the individual interfaces in the anodic and cathodic regions, cyclic voltammetry was carried out [43]. Figure 8 depicts the cyclic voltammograms of the fifth scan for EDLC fabricated using uncoated and coated electrodes. The electrode size is 1.5×3 cm² in the range 0–0.85 V and the scan rate is 1 mV s⁻¹. The shape of the voltammograms for the EDLCs with coated and uncoated electrodes is close to that of a rectangle. The electrolyte and the electrical contacts are responsible for the resistance of the EDLC. In the present polymer electrolyte system, ionic transport takes place in liquid phase entrapped in the polymer matrix. Therefore, the resistance value is expected to be high. Inset in Fig. 8 shows efficiency of the EDLC with PEG-coated electrodes for 100 cycles.

Fig. 7 Linear sweep voltammetry (LSV) curve of the 63.75 wt% MC-21.25 wt% NH_4NO_3 -15 wt% PEG

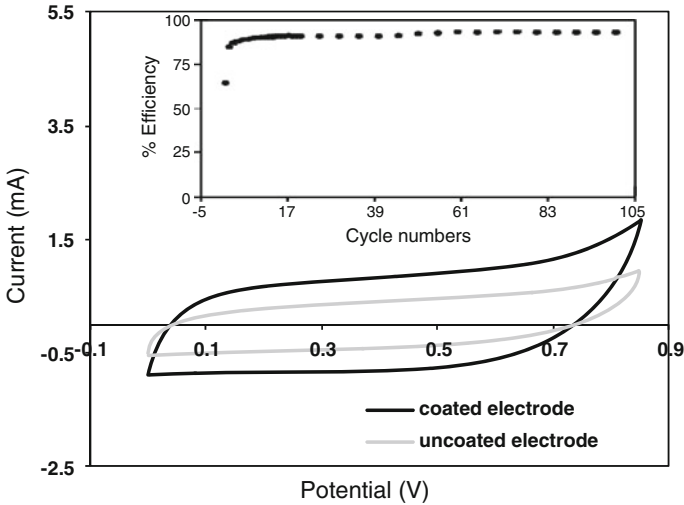
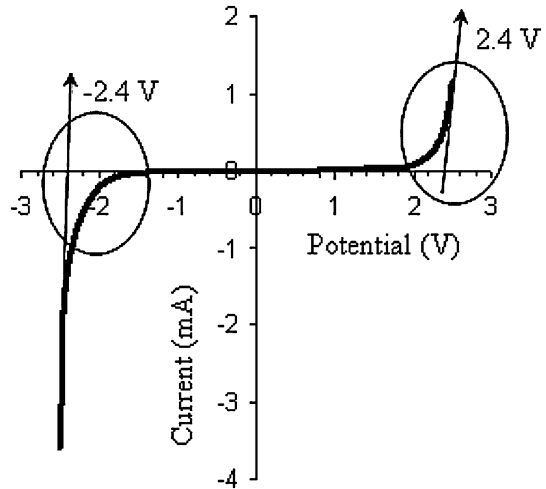


Fig. 8 Cyclic voltammogram of the EDLC fabricated using uncoated and coated electrodes. *Inset* efficiency of EDLC with PEG-coated electrodes for 100 cycles

Specific capacitance, C can be determined from cyclic voltammogram using the equation [44]:

$$C = \frac{i}{vm}$$

Here, i is the average current (A), v is the scan rate (V s^{-1}), and m is the weight of the electrode (g). The specific capacitance is listed in Table 3 for the two EDLCs.

The capacitance obtained with the 63.75 wt% MC-21.25 wt% NH_4NO_3 -15 wt% PEG electrolyte is higher than that fabricated EDLC using the unplasticized electrolyte as reported in our previous paper [3]. From CV test, the voltammograms

Table 3 Specific capacitance values for the EDLC obtained by cyclic voltammogram

| Electrodes | Charge capacitance [forward direction] (F g ⁻¹) | Discharge capacitance [reverse direction] (F g ⁻¹) |
|------------|--|---|
| Coated | 39 | 25 |
| Uncoated | 32 | 21 |

imply that, the fabricated EDLC using the plasticized 63.75 wt% MC-21.25 wt% NH₄NO₃-15 wt% PEG sample as electrolyte and activated carbon electrode depicts the capacitive behavior but the performance of the EDLC can still be improved to make the EDLC store and deliver charge in a shorter time. It can be observed that the EDLC with PEG-coated electrode showed higher charge and discharge capacitance. This is attributed to better contact between the electrode and electrolyte and should lead to a lower equivalent series resistance (ESR) compared to the EDLC with uncoated electrode.

Charge-discharge characteristics

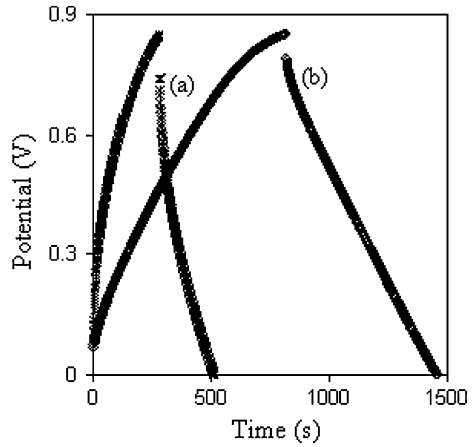
For EDLC performance, working voltage is largely dependent on the electrolyte breakdown voltage, while internal resistance and capacitance depends on the electrode resistance and conductivity of electrolyte. In this study, the voltage limits were set between 0 and 0.85 V and constant current of 1 mA was applied during charge and discharge. As reported in our previous paper [3], unplasticized MC-based electrolyte (75 wt% MC-25 wt% NH₄NO₃) with conductivity 2.10×10^{-6} S cm⁻¹ when used in a capacitor delivers low capacity of $\sim 1\text{--}2$ F g⁻¹. In this study, since the plasticized sample (63.75 wt% MC-21.25 wt% NH₄NO₃-15 wt% PEG) has conductivity 1.10×10^{-4} S cm⁻¹ (about two orders of magnitude higher), the capacitance of the fabricated EDLC should be higher. After studying the effect of PEG coating on the EDLC performance using CV, we now use the charge–discharge characteristics to evaluate the performance of the EDLC. Figure 9 shows the charge–discharge profile of the EDLCs fabricated.

From Fig. 9, it can be observed that, the discharge characteristics of the EDLC using coated electrodes is more linear compared to EDLC using uncoated electrodes. The linear curve shows the capacitive behavior of EDLC. The initial sudden jump/drop in the voltage while charging and discharging is due to ohmic loss across the internal resistance, equivalent circuit resistance (ESR) in electrode and electrolyte and represents the resistive behavior of EDLC [45]. ESR can be calculated from the voltage drop or IR_{drop} while discharging the EDLC as shown by the equation:

$$\text{ESR} = \frac{IR_{\text{drop}}}{i}$$

Here i is the discharge current and IR_{drop} is the voltage drop upon discharge. The specific capacitance can be evaluated from the gradient of the linear portion of the charge and discharge characteristics using the equation:

Fig. 9 Charge-discharge profile of the EDLCs for *a* uncoated and *b* coated electrodes



$$C_s = \frac{i \times \Delta t}{m \times \Delta V} = \frac{i}{m \times (\Delta V / \Delta t)}$$

Again *i* is the discharge current in amperes and $\Delta V / \Delta t$ is the gradient of the linear curve from charge-discharge profile ($V s^{-1}$). Gradient was obtained using trendline on the linear portion of the charge and discharge curves. The regression value was 0.99. Efficiency is one of the important parameters in EDLC performance. Efficiency, η was determined using the equation:

$$\eta = \frac{C_d}{C_c} \times 100\% = \frac{t_d}{t_c} \times 100\%$$

where C_d and C_c are discharge and charge capacitance, respectively. t_d represents the time for galvanostatic discharging and t_c represents the time for galvanostatic charging. Specific energy, *E* delivered during the discharge was calculated using the equation [46]:

$$E = \frac{1}{2} CV^2$$

Here, *C* is discharge capacitance and *V* is working voltage, 0.85 V. Power capability, *P* for EDLC can be determined using the equation:

$$P = \frac{V^2}{4R}$$

where *V* is working voltage, 0.85 V and *R* is internal resistance or ESR. Table 4 lists the value of equivalent series resistance (ESR), charge and discharge capacitance, efficiency, specific energy and power capability from EDLC studied evaluated from charge-discharge profile.

From Table 4, it can be deduced that, EDLC using coated electrodes give better performance compared to uncoated electrodes since, charge and discharge capacitance, efficiency, specific energy, and power delivered from EDLC using

coated electrodes are higher than EDLC with uncoated electrodes. CV results showed that ESR of the EDLC with PEG-coated electrode is lower to that of EDLC with uncoated electrodes and this has been confirmed from charge-discharge studies. Table 5 lists the comparison of the EDLC in this study with other reported studies. Exact comparison between results from this study and those of literature may not be possible because of different carbon materials and polymer electrolytes used. The basis of comparison is that in all the works quoted, SPEs are used.

Self-discharge characteristics

Self-discharge is one of the most crucial factors to determine the performance of the EDLC. It can be determined by measuring the open circuit voltage of the EDLC as a function of time. The EDLC cell was charged, discharged, and charged again at a constant current. When charging current is stopped, voltage decreased. This is self-discharge [50].

Table 4 Characteristic parameters for EDLC cells at 4th cycle for EDLC using uncoated and coated electrode

| Characteristics | Uncoated electrode | Coated electrode |
|---|--------------------|------------------|
| ESR (Ω) | 109 | 60 |
| Charge capacitance ($F\ g^{-1}$) | 31 | 42 |
| Discharge capacitance ($F\ g^{-1}$) | 25 | 38 |
| Coulombic efficiency (%) | 81 | 90 |
| Specific energy delivered ($W\ h\ kg^{-1}$) | 2.5 | 3.9 |
| Specific power delivered ($W\ kg^{-1}$) | 130 | 140 |

Table 5 Capacitance of EDLCs using different solid polymer electrolytes

| Polymer electrolytes | Electrode materials | Capacitance ($F\ g^{-1}$) | Ref[s] |
|--|---|-----------------------------|-----------|
| PEO ₂₅ -Mg(Tf) ₂ + 40 wt% EMITf | MWCNTs-AB-PVdF-HFP 70:10:20 (w/w) | 2.6–3.0 | [45] |
| Nafion/PTFE composite polymer | Carbon | 16 | [47] |
| (PEO-NPPP) ₁₁ /LiClO ₄ | 10 wt% carbon black Black Pearls 2000-PEO-NPPP | 17 | [48] |
| Polyvinyl alcohol–polystyrene sulphonic (3:7) | Carbon | 40 | [49] |
| 63.75 wt% MC-21.25 wt% NH ₄ NO ₃ -15 wt% PEG | PEG coated with activated carbon | 38 | This work |

PEO poly(ethylene oxide), *Mg(Tf)* magnesium trifluoromethanesulfonate, *EMITf* ionic liquid 1-ethyl-3-methylimidazolium trifluoromethanesulfonate, *MWCNTs* multiwalled-carbon nanotubes, *AB* acetylene black, *PVdF-HFP* poly(vinylidene fluoride-hexafluoropropylene), *PTFE* polytetrafluoroethylene, *NPPP* poly(propylene glycol)-*b*-poly(ethylene glycol)-*b*-poly(propylene glycol)-bis(2-aminopropyl ether), *LiClO₄* lithium perchlorate

Figure 10 demonstrates the voltage drop upon discharge at 1 mA compared to self-discharge (open circuit voltage) for EDLC using uncoated electrodes. It can be observed that the voltage initially dropped to 0.67 when the EDLC was discharged at 1 mA and 0.77 V for self-discharge.

Depicted in Fig. 11 is voltage drop upon discharge at 1 mA and open circuit voltage (OCV) for EDLC cell fabricated using PEG-coated electrode. The instantaneous voltage drop is related to internal resistance in EDLC. It can be observed that, the initial voltage drop for this cell when EDLC was discharged at 1 mA is 0.79 and 0.82 V for self-discharge. The voltage retention is better than that of the uncoated electrode EDLC. This again shows that PEG coating can upgrade the EDLC performance.

It may be concluded that the MC-based electrolyte can be used as an electrolyte in an EDLC. However, more work needs to be carried out to improve performance of EDLC using MC-based electrolytes.

Fig. 10 Self-discharge profiles resulting from charging EDLC to 0.85 V using uncoated electrodes

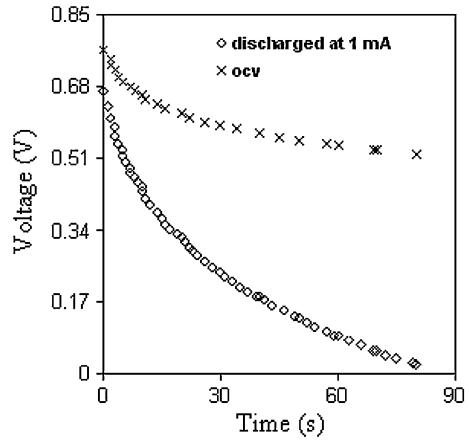
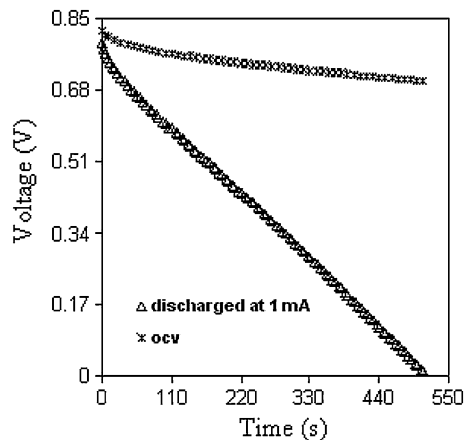


Fig. 11 Self-discharge profile resulting from charging EDLC to 0.85 V using coated electrodes



Conclusions

FTIR studies show that, MC, NH_4NO_3 , and PEG have interacted from the shifting of C–O stretching mode. From EIS measurements, the 63.75 wt% MC-21.25 wt% NH_4NO_3 -15 wt% PEG sample can be represented by the equation:

$$Z_{\text{total}} = R + \frac{k}{\omega^p} [\cos(p\pi/2) - j \sin(p\pi/2)]$$

The specific discharge capacitance is 38 F g^{-1} obtained from the EDLC with PEG-coated electrodes. From LSV test, it was found that MC-based polymer electrolytes have high-electrochemical stability, 2.4 V and safe to use as a membrane in EDLC that is charged to below the decomposition voltage. CV voltammogram shows that EDLC with PEG-coated electrode has higher capacitance compared to EDLC with uncoated electrodes. EDLC using coated electrode with PEG gives better performance compared to uncoated electrode implying that coating the electrode with PEG helps to improve electrode-electrolyte contact.

Acknowledgments The authors would like to acknowledge University of Malaya for providing financial support (PS223/2008C and PS312/2009C) and to the Ministry of Higher Education Malaysia (MOHE) for grant awarded (FP048/2008C).

References

- Gualous H, Bouquain D, Berthon A, Kauffmann JM (2003) Experimental study of supercapacitor serial resistance and capacitance variations with temperature. *J Power Sour* 123:86–93
- Tanahashi I (2005) Comparison of the characteristics of electric double-layer capacitors with an activated carbon powder and an activated carbon fiber. *J Appl Electrochem* 35:1067–1072
- Shuhaimi NEA, Majid SR, Arof AK (2009) On complexation between methyl cellulose and ammonium nitrate. *Mater Res Innovat* 13:239–242
- Shuhaimi NEA, Teo LP, Majid SR, Arof AK (2010) Transport studies of NH_4NO_3 doped methyl cellulose electrolyte. *Synth Met* 160:1040–1044
- Shuhaimi NEA, Alias NA, Kufian MZ, Majid SR, Arof AK (2010) Characteristics of methyl cellulose- NH_4NO_3 -PEG electrolyte and application in fuel cells. *J Solid State Electrochem* 14:2153–2159
- García MA, Pinotti A, Martino M, Zaritzky N (2009) Electrically treated composite FILMS based on chitosan and methylcellulose blends. *Food Hydrocolloid* 23:722–728
- Filho GR, de Assunção RMN, Viera JG, Meireles CS, Cerqueira DA, da Silva Barud H, Ribeiro SJL, Messaddeq Y (2007) Characterization of methylcellulose produced from sugar cane bagasse cellulose: crystallinity and thermal properties. *Polym Degrad Stab* 92:205–210
- Ozeki T, Yuasa H, Okada H (2005) Controlled release of drug via methylcellulose-carboxyvinylpolymer interpolymer complex solid dispersion. *AAPS PharmSciTech* 6:E231–E236
- Yin J, Luo K, Chen X, Khutoryanskiy VV (2006) Miscibility studies of the blends of chitosan with some cellulose ethers. *Carbohydr Polym* 63:238–244
- Gotoh Y, Fujimura K, Ohkoshi Y, Nagura M, Akamatsu K, Shigehito D (2004) Preparation of transparent alumina film and fiber from a composite of aluminum polynuclear complex/methyl cellulose. *Mater Chem Phys* 83:54–59
- Park JS, Ruckenstein E (2001) Viscoelastic properties of plasticized methylcellulose and chemically crosslinked methylcellulose. *Carbohydr Polym* 46:373–381
- Lin S-Y, Wang S-L, Wei Y-S, Li M-J (2007) Temperature effect on water desorption from methylcellulose films studied by thermal FT-IR microspectroscopy. *Surf Sci* 601:781–785
- Ramya CS, Selvasekarapandian S, Savitha T (2008) Proton-conducting membranes: poly (*N*-vinyl pyrrolidone) complexes with various ammonium salts. *J Solid State Electrochem* 12:807–814

14. Kumar M, Sekhon SS (2002) Role of plasticizer's dielectric constant on conductivity modification of PEO-NH₄F polymer electrolytes. *Eur Polym J* 38:1297–1304
15. Binesh N, Bhat SV (1996) Concentration-dependent NMR and conductivity studies of (PEG)_xNH₄ClO₄. *Solid State Ionics* 92:261–264
16. Qian X, Gu N, Cheng Z, Yang X, Wang E, Dong S (2001) Impedance study of (PEO)₁₀LiClO₄-Al₂O₃ composite polymer electrolyte with blocking electrodes. *Electrochim Acta* 46:1829–1836
17. Xu W, Siow KS, Gao Z, Lee SY (1998) A.C. impedance study on the interface of lithium and polymer electrolyte based on lithium-*N*(4-sulfophenyl) malaeimide. *Solid State Ionics* 112:1–8
18. Latham RJ, Rowlands SE, Schlindwein WS (2002) Supercapacitors using polymer electrolytes based on poly(urethane). *Solid State Ionics* 147:243–248
19. Chang J-K, Shong D-NS, Tsai W-T (2003) Effects of alloying elements and binder on the electrochemical behavior of metal hydride electrodes in potassium hydroxide electrolyte. *J Solid State Electrochem* 7:485–491
20. Bispo-Fonseca I, Aggar J, Sarrazin C, Simon P, Fauvarque JF (1999) Possible improvements in making carbon electrodes for organic supercapacitors. *J Power Sour* 79:238–241
21. Kolhe P, Kannan RM (2003) Improvement in ductility of chitosan through blending and copolymerization with PEG: FTIR investigation of molecular interactions. *Biomacromolecules* 4:173–180
22. Rajendran S, Babu RS, Sivakumar P (2007) Effect of salt concentration on poly(vinyl chloride)/poly(acrylonitrile) based hybrid polymer electrolytes. *J Power Sour* 170:460–464
23. Liu W, Zhang B, Lu WW, Li X, Zhu D, Yao DK, Wang Q, Zhao C, Wang C (2004) A rapid temperature-responsive sol-gel reversible poly(*N*-isopropylacrylamide)-*g*-methylcellulose copolymer hydrogel. *Biomaterials* 25:3005–3012
24. Pinotti A, Garcia MA, Martino MN, Zaritzky NE (2007) Study on microstructure and physical properties of composite films based on chitosan and methylcellulose. *Food Hydrocolloid* 21:66–72
25. Rimdusit S, Jingjind S, Damrongsakkul S, Tiptipakorn S, Takeichi T (2008) Biodegradability and property characterizations of methyl cellulose: effect of nanocompositing and chemical crosslinking. *Carbohydr Polym* 72:444–455
26. Ramya CS, Selvasekarapandian S, Hirankumar G, Savitha T, Angelo PC (2008) Investigation on dielectric relaxations of PVP-NH₄SCN polymer electrolyte. *J Non-Crystalline Solids* 354:1494–1502
27. Majid SR (2007) High polymer weight chitosan as polymer electrolyte for electrochemical devices. Dissertation, University of Malaya, Kuala Lumpur
28. Hashmi SA, Kumar A, Maurya KK, Chandra S (1990) Proton-conducting polymer electrolyte 1: the polyethylene oxide + NH₄ClO₄ system. *J Phys D Appl Phys* 23:1307–1314
29. Singh HP, Kumar R, Sekhon SS (2005) Correlation between ionic conductivity and fluidity of polymer gel electrolytes containing NH₄CF₃SO₃. *Bull Mater Sci* 28:467–472
30. Marinković NS, Calvente JJ, Kloss A, Kováčová Z, Fawcett WR (1999) SNIFTIRS studies of the electrochemical double layer Part II. Au(111) electrode in solutions with specifically adsorbed nitrate ions. *J Electroanal Chem* 467:325–334
31. Zhang J, Han F, Wei X, Shui L, Gong H, Zhang P (2010) Spectral studies of hydrogen bonding and interaction in the absorption processes of sulfur dioxide in poly(ethylene glycol) 400 + water binary system. *Ind Eng Chem Res* 49:2025–2030
32. Fang C, Bhattarai N, Sun C, Zhang M (2009) Functionalized nanoparticles with long-term stability in biological media. *Small* 5:1637–1641
33. Deng Y, Dixon JB, White GN (2006) Bonding mechanisms and conformation of poly(ethylene oxide)-based surfactants in interlayer of smectite. *Colloid Polym Sci* 284:347–356
34. Ayranci E, Tunc S (1997) Cellulose-based edible films and their effects on fresh beans and strawberries. *Z Lebensm Unters Forsch A* 205:470–473
35. Park MK, Kim HS, An JH, Kim J (2005) New oligomeric ether plasticizers for solid polymer electrolytes: Synthesis and electrical properties of oligomeric PEO having bis(five-membered cyclic carbonate)s at chain ends. *J Ind Eng Chem* 11:222–227
36. Subban RHY, Ahmad AH, Kamarulzaman N, Ali AMM (2005) Effects of plasticiser on the lithium ionic conductivity of polymer electrolyte PVC-LiCF₃SO₃. *Ionics* 11:442–445
37. Pradhan DK, Choudhary RNP, Samantaray BK, Karan NK, Katiyar RS (2007) Effect of plasticizer on structural and electrical properties of polymer nanocomposite electrolytes. *Int J Electrochem Sci* 2:861–871
38. Srivastava N, Chandra S (2000) Studies on a new proton conducting polymer system: poly(ethylene succinate) + NH₄ClO₄. *Eur Polym J* 36:421–433

39. Wu GM, Lin SJ, Yang CC (2006) Preparation and characterization of PVA/PPA membranes for solid polymer electrolytes. *J Membr Sci* 275:127–133
40. Lee CH, Park HB, Lee YM, Lee RD (2005) Importance of proton conductivity measurement in polymer electrolyte membrane for fuel cell application. *Ind Eng Chem Res* 44:7617–7626
41. Han DG, Choi GM (1998) Computer simulation of the electrical conductivity of composites: the effect of geometrical arrangement. *Solid State Ionics* 106:71–87
42. Gerbaldi C, Nair JR, Meligrana G, Bongiovanni R, Bodoardo S, Penazzi N (2009) Highly ionic conducting methacrylic-based gel-polymer electrolytes by UV-curing technique. *J Appl Electrochem* 39:2199–2207
43. Hashmi SA, Kumar A, Tripathi SK (2007) Experimental studies on poly methyl methacrylate based gel polymer electrolytes for application in electrical double layer capacitors. *J Phys D* 40:6527–6534
44. Chandrasekaran R, Soneda Y, Yamashita J, Kodama M, Hatori H (2008) Preparation and electrochemical performance of activated carbon thin films with polyethylene oxide-salt addition for electrochemical capacitor applications. *J Solid State Electrochem* 12:1349–1355
45. Pandey GP, Kumar Y, Hashmi SA (2011) Ionic liquid incorporated PEO based polymer electrolyte for electrical double layer capacitors: a comparative study with lithium and magnesium systems. *Solid State Ionics* 190:93–98
46. Wei Y-Z, Fang B, Iwasa S, Kumagai M (2005) A novel electrode material for electric double-layer capacitors. *J Power Sour* 141:386–391
47. Subramaniam CK, Ramya CS, Ramya K (2011) Performance of EDLCs using Nafion and Nafion composites as electrolyte. *J Appl Electrochem* 41:197–206
48. Lavall RL, Borges RS, Calado HDR, Welter C, Trigueiro JPC, Rieumont J, Neves BRA, Silva GG (2008) Solid state double layer capacitor based on a polyether polymer electrolyte blend and nanostructured carbon black electrode composites. *J Power Sour* 177:652–659
49. Kumar MS, Bhat DK (2009) Polyvinyl alcohol-polystyrene sulphonic acid blend electrolyte for supercapacitor application. *Phys B* 404:1143–1147
50. Ricketts BW, Ton-That C (2000) Self-discharge of carbon-based supercapacitors with organic electrolytes. *J Power Sour* 89:64–69